

# Superconductivity Near a Quantum Critical Point: Bounds on the Transition Temperature in the $\gamma$ -Model

Ahmed Elezaby and Artem Abanov

*Department of Physics and Astronomy, Texas A&M University, College Station, TX 77843, USA*

(Dated: December 24, 2025)

Near a quantum critical point (QCP) in a metal, strong Fermion-Fermion interactions mediated by soft collective bosons give rise to two competing phenomena: non-Fermi liquid behavior and superconductivity that deviates from conventional BCS and Migdal-Eliashberg theories. We consider the problem of obtaining closed-form analytical lower and upper bounds on transition temperatures for such systems. We focus mainly on a class of models known as the  $\gamma$ -model, which generalizes the Eliashberg theory of Superconductivity where the effective interaction potential scales as  $V(\Omega) \propto 1/|\Omega|^\gamma$ . Building on a recent reformulation of Migdal-Eliashberg theory—expressed as a classical infinite spin chain with nonlocal interactions [1, 2]—and employing a simple linear algebra framework, we derive rigorous closed-form expressions for upper and lower bounds on the superconducting transition temperature for any  $\gamma > 0$ . While our lower bounds coincide precisely with those previously in the literature [3], our derivation offers a more streamlined and accessible method. Moreover, our upper bounds are substantially tighter than any existing estimates and converge rapidly enough to the numerical results from various prior studies.

## I. INTRODUCTION

Superconductivity is a macroscopic quantum state of matter in which certain materials exhibit precisely zero electrical resistance when cooled below a characteristic critical temperature,  $T_c$ . The field's origin traces back to 1911, when Dutch physicist H. Kamerlingh Onnes, in his quest to understand the behavior of matter near absolute zero, first observed superconductivity in mercury [4]. This landmark discovery was enabled by his earlier success in liquefying helium in 1908 [5], which provided the cryogenic environment necessary to reach 4.2 K. At this temperature, Onnes found that the electrical resistance of his mercury sample vanished completely. Another defining feature is perfect diamagnetism below  $T_c$ , known as Meissner effect, and was discovered in 1933 by Walther Meissner and Robert Ochsenfeld [6]. This demonstrated that superconductivity is a true thermodynamic equilibrium state, not merely a dynamic state of infinite conductivity, thereby revealing the deep quantum mechanical nature of the phenomenon.

The first successful theoretical microscopic description came more than 20 years later by Bardeen, Cooper, and Schrieffer (BCS) [7, 8]. BCS theory's key idea is that a phonon-mediated effective attraction overcomes the Coulomb repulsion, binding electrons into Cooper pairs [7, 8]. These pairs, being bosonic, condense into a single macroscopic quantum state, protected by an energy gap ( $\Delta$ ), which is responsible for the system's remarkable properties. BCS theory was a monumental success, explaining the energy gap, the  $T_c$  formula, the specific heat jump, and the isotope effect [9, 10].

Despite its success, BCS is a weak-coupling theory. It was generalized by Eliashberg (building on work by Migdal [11]) in 1960 to handle the strong-coupling regime, where the electron-phonon interaction is large [12, 13]. Eliashberg theory explicitly accounts for the retardation of the phonon-mediated interaction—the fact

that the lattice response (phonons) is much slower than the electronic motion. This strong-coupling theory, which requires solving a set of coupled integral equations, provided a quantitative description for materials like lead and mercury, where BCS theory failed numerically.

This phonon-mediated paradigm reigned until 1986, with the discovery of high- $T_c$  superconductivity in cuprates by Bednorz and Müller [14]. The transition temperatures observed (eventually exceeding 130 K) were far beyond what was believed possible within the phonon-mediated Eliashberg framework [15, 16]. This discovery ushered in the era of unconventional superconductivity. These materials, and subsequently others like iron-based pnictides [17] and heavy-fermion compounds [18], share a common trait: superconductivity often emerges on the border of another ordered phase, typically antiferromagnetism. This proximity to a magnetic phase suggests a different pairing mechanism. Instead of phonons, the glue binding the Cooper pairs is thought to be the collective fluctuations of the competing order. When this competing order (e.g., magnetism) is tuned to zero temperature by a non-thermal parameter (like pressure, doping, or magnetic field), a Quantum Critical Point (QCP) is realized [19]. At a QCP, the system is dominated by scale-invariant quantum fluctuations. These gapless, critical fluctuations (e.g., spin fluctuations) provide a powerful, universal pairing interaction [20, 21].

This new paradigm presents profound theoretical challenges. The pairing interaction is no longer gapped. There is no large energy scale separation that allowed for the Copper logarithm to be the major contribution. The bosonic mode cannot be regarded as slow, causing a breakdown of Migdal's theorem, which is fundamental to Eliashberg theory. The system's normal state is often a "strange metal" or non-Fermi liquid, lacking the well-defined quasiparticles that form the basis of BCS [22]. The so-called "gamma model" (or  $\gamma$ -model) has emerged as a key theoretical framework to address this

regime [23–30]. It simplifies the problem by modelling the pairing interaction mediated by these critical fluctuations with a phenomenological, singular frequency dependence:  $V(\Omega) \propto 1/|\Omega|^\gamma$ . The exponent  $\gamma$  parameterizes the nature of the critical fluctuations. This model allows for a focused study of how a singular interaction gives rise to superconductivity and determines  $T_c$ , bridging the gap between quantum criticality and pairing.

For a list of quantum-critical materials that are effectively described by the  $\gamma$ -model, we refer the reader to [25].

### A. Universality of the $\gamma$ -Model

The  $\gamma$ -model is not just an abstract mathematical construct; it also provides a mathematical bridge, with the exponent  $\gamma$  acting as a tuning parameter that can recover the essential mathematical structures and physical properties of both BCS and Eliashberg theories. The BCS model assumes a frequency-independent (non-retarded) interaction,  $V(\Omega) = V_0$ , which is active up to a cutoff  $\omega_D$ . This is mathematically equivalent to setting  $\gamma = 0$  in the gamma model,  $V(\Omega) \propto 1/|\Omega|^0 = \text{constant}$ . In this limit, the gamma model's gap equation (with an appropriate cutoff) reduces to the BCS gap equation. The  $T_c$  calculation then yields the famous non-perturbative BCS formula,  $T_c \propto \omega_D \exp(-1/\lambda)$ , where  $\lambda$  is the dimensionless electron-phonon coupling constant.

The standard Eliashberg theory for phonon-mediated superconductivity is a fully retarded theory. The electron-phonon kernel  $\lambda(\Omega)$  (which describes the interaction) decays rapidly at high frequencies. Specifically, for  $\Omega \gg \omega_D$  (the maximum phonon frequency), the kernel has the asymptotic behavior  $\lambda(\Omega) \propto 1/\Omega^2$ . This is precisely the case of the gamma model with  $\gamma = 2$ . This value represents a safe case where the Matsubara sums converge quickly, just as they do in Eliashberg theory. Thus, the  $\gamma = 2$  model captures the essential mathematical character (the convergence and scaling) of the conventional, retarded phonon-pairing problem. The gamma model, therefore, interpolates between the non-retarded BCS-like problem ( $\gamma = 0$ ) and the retarded Eliashberg-like problem ( $\gamma = 2$ ). It also generalizes to different retarded and non-retarded regimes for different values of  $\gamma$ , providing a universal framework that describes general quantum critical behavior, not just quantum critical superconductivity.

For any  $\gamma > 0$ , the gamma model requires no upper frequency cutoff. As such, the model has only one energy scale — the bare electron-boson coupling constant  $g$ . As a consequence, every other energy scale, such as  $\Delta$  or  $T_c$  must have a form  $gf(\gamma)$ , where  $f(\gamma)$  is a universal function of the dimensionless parameter  $\gamma$ . This simple observation makes the gamma model a universal model of a metal's behaviour at QCP.

A recent framework for analyzing the strong-coupling Migdal-Eliashberg theory, and its  $\gamma$ -model generaliza-

tion, was developed in the work of Ref. [1, 2], where the theory was mapped onto a classical spin chain with long-range Heisenberg exchange and Zeeman terms. In this representation, the discrete fermionic Matsubara frequencies,  $\omega_m = (2m + 1)\pi T$ , become the sites of a one-dimensional chain. A three-component classical spin vector,  $\mathbf{S}_m$ , is placed at each site, with its orientation encoding the properties of the superconducting order parameter at that frequency. This reduces the problem of solving complex integral equations to the optimization of a well-defined free energy functional, expressed entirely in terms of these spin variables. Within this framework, the analysis becomes significantly more tractable; in particular, the critical transition temperatures, which mark the instability of the normal state, are identified by performing a linear stability analysis. This translates directly to calculating the eigenvalues of the Hessian matrix (the second functional derivative) of the free energy. A transition occurs when an eigenvalue crosses zero, signalling the emergence of a new superconducting state. As we shall show in Sec. II, the linearized Hessian matrix  $H$  at the normal state reads:

$$H_{nn} = (2n + 1)\tau^\gamma + 2 \sum_{m=1}^n \frac{1}{m^\gamma} - \frac{1}{(2n + 1)^\gamma}, \quad (1)$$

and for  $m \neq n$ :

$$H_{mn} = - \left( \frac{1}{|m - n|^\gamma} + \frac{1}{(m + n + 1)^\gamma} \right). \quad (2)$$

Where  $\tau \equiv \frac{2\pi T}{g}$  is the dimensionless temperature, and  $g$  is the bare coupling constant. Notice the remarkable absence of any parameters except dimensionless  $\gamma$  and  $\tau$ , which allows for calculation of the transition temperature as a function of  $\gamma$  only. The normal state is a minimum when all eigenvalues of the Hessian are positive. It becomes a saddle point when one of the eigenvalues changes sign. This is where the superconducting transition happens.

To analyze the eigenvalues numerically, we need to truncate the linear Hessian matrix to a finite  $N \times N$  matrix. The size  $N$  should be such that the Zeeman field overwhelms the interaction near the end of the chain as it does at large Matsubara frequencies in an infinite chain. This translates into the requirement  $N \gg \tau^{-\gamma}$  for  $\gamma > 1$  and  $(N\tau)^\gamma \gg 1$  for  $\gamma < 1$  [2]. However, while this approach is both numerically and computationally practical, it presents two key subtleties that must be addressed before it can be reliably applied:

- **Infinite-dimensional Hessian matrix:** The Hessian matrix in question is infinite-dimensional, with diagonal elements  $H_{nn} \rightarrow \infty$  as  $n \rightarrow \infty$  for any  $\gamma > 0, \tau > 0$ . This implies that the matrix  $H$  is neither compact nor bounded. Consequently, truncating it to a finite  $N \times N$  matrix is not trivially justified and must be done carefully.

- **Dependence on prior knowledge of the transition temperature:** Even if truncation were feasible, the conditions  $N \gg \tau^{-\gamma}$  for  $\gamma > 1$  and  $(N\tau)^\gamma \gg 1$  for  $\gamma < 1$  require prior knowledge of the transition temperature  $\tau_c$ , or at least its bounds. This creates a circular dependency: one needs to know  $\tau_c$  to determine the truncation size necessary to compute  $\tau_c$ . While previous studies have estimated the transition temperature using alternative methods [25–31], a self-contained approach based on the spin chain mapping only would be more comprehensive.

These issues were recently addressed by the original authors of the spin chain mapping approach [3, 32, 33]. They introduced a compact, self-adjoint operator  $\mathfrak{B}(\gamma)$ , identifying the transition temperature as (see Eq. (46) in [3]):

$$T_c = \frac{1}{2\pi} [\mathfrak{g}(\gamma)]^{\frac{1}{\gamma}},$$

where  $\mathfrak{g}(\gamma)$  is the largest eigenvalue of  $\mathfrak{B}(\gamma)$ . They introduced a variational method to derive lower bounds on this eigenvalue, and hence on the transition temperature, and used fixed-point theory to establish an upper bound.

While their results are mathematically rigorous, they are primarily tailored to a mathematically inclined audience. Moreover, the upper bound they derive is exceedingly high, even for large values of  $\gamma$  and does not converge rapidly enough to the lower bound or to the numerical data, suggesting a potential for improvement. Our work aims to address these two points. We build on their mathematical argument and show that it's possible to establish a truncation for the original Hessian matrix without the need for introducing a new matrix. We also show that, using a simple linear algebra framework and even when taking the limit  $N \rightarrow \infty$ , we can establish sharper upper bounds.

## B. Overview of our results

The main results of this work can be summarized in the following points:

- We showed that it's both mathematically possible, and physically justifiable to truncate the infinite Hessian matrix to a finite  $N \times N$  for the purpose of finding the transition temperature, i.e when a negative eigenvalue appears.
- Increasing the size  $N$  will increase the accuracy of the transition temperature calculation. We calculate the exact temperatures for the sizes  $N = 1, 2, 3, 4$  which can be taken as progressing lower bounds approaching the actual temperature from below. In these cases, the  $N$ -th bound is obtained as the smallest positive solution of the equation

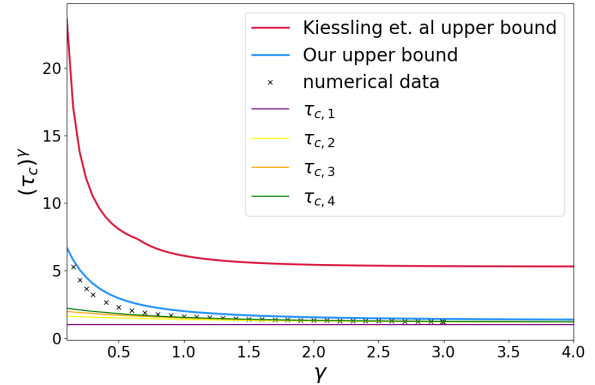


FIG. 1. Our results for the first four lower bounds  $\tau_{c,1}^\gamma, \tau_{c,2}^\gamma, \tau_{c,3}^\gamma, \tau_{c,4}^\gamma$  as obtained from Eq.s (32),(35),and(36), and our upper bound calculated from Eq (44) in comparison with the numerical data from [31] and the upper bound obtained by Kiessling et al [3]. Note that we are plotting  $\tau^\gamma$  instead of  $\tau$  vs  $\gamma$ .

$\det(H^{(N)}) = 0$  equation where  $H^{(N)}$  is the  $N \times N$  truncation of the Hessian matrix. Our analytical results agree identically with those of Kiessling et. al [3] and works as lower bounds for numerical results obtained before.

- We establish a significantly improved upper bound on the transition temperature using Gershgorin circle theorem and by scaling the original Hessian matrix through a similarity transformation. This sharpens the bound on the eigenvalues of the Hessian in terms of the matrix entries, which enables us to establish a bound on the transition temperature  $\tau_c$ .

Our results are summarized in Fig. 1.

## C. Structure of the paper

The paper is structured as follows. In section II we review the  $\gamma$ -model and its mapping to a classical spin chain. We derive the gap equation and the Hessian matrix needed to do our analysis. In section III, we present the mathematical argument for the truncation of the Hessian matrix. Section IV introduces the lower bounds for the transition temperatures using the Interlacing Eigenvalue theorem. In section V, we use the Gershgorin Circle theorem to establish an upper bound for the transition temperature. Summary and the conclusions are presented in the section VI.

## II. THE $\gamma$ -MODEL

Pairing near a Quantum Critical Point (QCP) arises from a mechanism fundamentally different from that of conventional BCS theory [31, 34]. In this regime, the effective dynamic electron-electron interaction  $V(\mathbf{q}, \Omega)$  is mediated by a critical collective bosonic mode. The condensation of this boson at the QCP provides strong attraction in one or more pairing channels. Simultaneously, it induces non-Fermi liquid (NFL) behavior in the normal state. These two tendencies—pairing and NFL behavior—compete, and determining which dominates requires analyzing a set of coupled nonlinear integral equations for the fermionic self-energy  $\Sigma(\mathbf{k}, \omega)$  and the gap function  $\Delta(\mathbf{k}, \omega)$ , where  $\mathbf{k}$  and  $-\mathbf{k}$  are the momenta of paired fermions and  $\omega$  is the Matsubara frequency.

We consider a class of models in which the collective bosons are slow modes compared to the dressed fermions, due to various physical reasons. In this limit, the self-energy and pairing vertex can be approximated by their values on the Fermi surface, similar to the treatment in the standard Eliashberg theory [12, 13, 35].

A key feature of the  $\gamma$ -model is that the effective dynamical interaction takes the form  $V(\Omega_m) \propto 1/|\Omega_m|^\gamma$ , where  $\Omega_m$  is the transferred bosonic Matsubara frequency. Near the QCP, the fermion-boson interaction becomes infinitely strong. In this limit, the only remaining energy scale in the problem is the bare fermion-boson coupling strength, denoted by  $g$  in this paper. As a result, the system becomes universal, with its behavior governed solely by the nature of the bosonic mode, encapsulated in the dimensionless parameter  $\gamma$ . This universality is what defines the  $\gamma$ -model.

### A. Generalized Eliashberg Equations

Near a Quantum Critical Point (QCP), the bosonic gap vanishes, and the bosonic propagator takes the form:

$$\chi(\omega) \sim |\omega|^{-\gamma}, \quad (3)$$

where  $\gamma > 0$  is a dimensionless parameter that depends on the nature of the QCP.

The generalized Eliashberg equations for arbitrary  $\gamma$  can be derived in the Matsubara formalism. They are given by [23, 25–30]: (the Matsubara frequencies  $\omega_m = \pi T(2m+1)$ , the anomalous vertex  $\Phi_n \equiv \Phi(\omega_n)$ , and the electron self-energy  $\Sigma_m \equiv \Sigma(\omega_m)$ )

$$\Phi_m = g^\gamma \pi T \sum_{m' \neq m} \frac{\Phi_{m'}}{\sqrt{\Sigma_{m'}^2 + \Phi_{m'}^2}} \frac{1}{|\omega_m - \omega_{m'}|^\gamma}, \quad (4)$$

and

$$\Sigma_m = \omega_m + g^\gamma \pi T \sum_{m' \neq m} \frac{\Sigma_{m'}}{\sqrt{\Sigma_{m'}^2 + \Phi_{m'}^2}} \frac{1}{|\omega_m - \omega_{m'}|^\gamma}. \quad (5)$$

The superconducting gap function  $\Delta_m$  is defined as:

$$\Delta_m = \omega_m \frac{\Phi_m}{\Sigma_m}. \quad (6)$$

Substituting this into the equations above, we obtain a single self-consistent equation for the gap function:

$$\Delta_m = g^\gamma \pi T \sum_{m' \neq m} \frac{\Delta_{m'} - \Delta_m \frac{\omega_{m'}}{\omega_m}}{\sqrt{\omega_{m'}^2 + \Delta_{m'}^2}} \frac{1}{|\omega_m - \omega_{m'}|^\gamma}. \quad (7)$$

This equation involves only the gap function  $\Delta(\omega_m)$ , but it appears on both sides, making it a nonlinear summation equation that must be solved self-consistently.

### B. Mapping to the Classical Spin Chain

In [1], the Migdal–Eliashberg theory of superconductivity was mapped onto a classical Heisenberg spin chain in a Zeeman magnetic field, where the lattice sites correspond to Fermionic Matsubara frequencies  $\omega_m$ . In terms of classical spin variables  $\mathbf{S}_m$ , the Holstein Hamiltonian  $H_s$  can be written as:

$$H_s(\omega_m) = -2\pi \sum_m \omega_m S_m^z - g^2 \pi^2 T \sum_{m' \neq m} \frac{\mathbf{S}_m \cdot \mathbf{S}_{m'} - 1}{|\omega_m - \omega_{m'}|^\gamma}, \quad (8)$$

where  $T$  is the temperature and  $g$  is the electron-phonon coupling constant.

Introducing the frequency-dependent gap function  $\Delta_m \equiv \Delta(\omega_m)$  through the spin components:

$$S_m^z = \frac{\omega_m}{\sqrt{\omega_m^2 + |\Delta_m|^2}}, \quad S_m^+ = \frac{\Delta_m}{\sqrt{\omega_m^2 + |\Delta_m|^2}}, \quad (9)$$

where  $S_m^+ = S_m^x + iS_m^y$ .

It was shown in [1, 2] that, with an appropriate choice of the overall phase, the gap function at the free energy minimum satisfies the following properties:

- $\Delta_m \geq 0$  for all  $\omega_m$ ,
- $\Delta_m$  is an even function of  $\omega_m$ ,
- $\Delta_m \rightarrow 0$  as  $\omega_m \rightarrow \pm\infty$ .

These properties also hold in the zero-temperature limit  $T = 0$ , where  $\omega_m$  becomes a continuous variable  $\omega$ .

From these properties, it follows that  $S_m^y = 0$  and  $S_m^x \geq 0$ . Let  $\theta_m$  be the angle between  $\mathbf{S}_m$  and the  $z$ -axis. Then:

$$S_m^z = \cos \theta_m, \quad S_m^x = \sin \theta_m, \quad 0 \leq \theta_m \leq \pi.$$

The gap function can then be expressed as:

$$\Delta_m = \omega_m \tan \theta_m, \quad (10)$$

subject to the boundary conditions:

$$\theta(-\omega_m) = \pi - \theta(\omega_m), \quad \lim_{\omega_m \rightarrow \pm\infty} \theta_m = n\pi, \quad n \in \mathbb{Z}. \quad (11)$$

In terms of the angles  $\theta_m$ , the spin chain Hamiltonian becomes [2]:

$$H_s(\theta_m) = -2\pi \sum_m \omega_m \cos \theta_m - g^\gamma \pi^2 T \sum_{m' \neq m} \frac{\cos(\theta_m - \theta_{m'}) - 1}{|\omega_m - \omega_{m'}|^\gamma}. \quad (12)$$

Differentiating with respect to  $\theta_m$ , we obtain the equation for stationary points of the  $\gamma$ -model:

$$\omega_m \sin \theta_m = g^\gamma \pi T \sum_{m' \neq m} \frac{\sin(\theta_m - \theta_{m'})}{|\omega_m - \omega_{m'}|^\gamma}. \quad (13)$$

Comparing this with Eq. (7), we see that this is indeed the superconducting gap equation expressed in terms of the angles  $\theta_m$ .

### C. Boundary Conditions

From Eq. (13), we can rewrite the equations as:

$$\sin \theta_m = \frac{g^\gamma \pi T}{(2m+1)} \sum_{m' \neq m} \frac{\sin(\theta_m - \theta_{m'})}{|m - m'|^\gamma}. \quad (14)$$

For  $\gamma > 1$ , the summation in right-hand side of Eq. (14) converges since  $|\sin(\theta_m - \theta_{m'})| \leq 1$  and  $\sum_{n=1}^{\infty} \frac{1}{n^\gamma}$  converges for  $\gamma > 1$ . This implies that  $\theta_m \rightarrow 0$  as  $m \rightarrow \infty$ .

The analysis for  $\gamma \leq 1$  is complicated by the non-convergence of the summation. Physically, however, we require the system to exhibit asymptotic behavior analogous to that of a large finite chain, where high Matsubara frequencies make vanishingly small contributions to the gap function. Mathematically, the limit  $\lim_{m \rightarrow \infty} \theta_m = 0$  is a necessary, though not sufficient, condition; while it admits a solution to the gap equation, it does not guarantee uniqueness. In the following analysis, we impose this boundary condition for all  $\gamma > 0$ . We utilize this condition primarily to justify the assumption of discrete negative eigenvalues for the Hessian matrix—a property that will hold strictly for  $\gamma > 1$ . Consequently, our central assumption for the regime  $0 < \gamma \leq 1$  is that, under this boundary condition, the calculation of the transition temperature's upper limit remains valid using an untruncated infinite matrix ( $N \rightarrow \infty$ ). The validity of this approach is supported by the close agreement between our results and numerical data from prior studies.

### D. The Free Energy Functional and the Hessian Matrix

From the definition of the Fermionic Matsubara frequency  $\omega_m = (2m+1)\pi T$ , the Hamiltonian exhibits the following symmetries:

$$\omega_{-m-1} = -\omega_m, \quad \theta_{-m-1} = \pi - \theta_m. \quad (15)$$

These symmetries allow us to express the Hamiltonian using only non-negative indices  $m \geq 0$ :

$$H_s = -4\pi \sum_{m=0}^{\infty} \omega_m \cos \theta_m - 2g^\gamma \pi^2 T \sum_{\substack{n,m=0 \\ n \neq m}}^{\infty} \frac{\cos(\theta_m - \theta_n) - 1}{|\omega_m - \omega_n|^\gamma} + 2g^\gamma \pi^2 T \sum_{n,m=0}^{\infty} \frac{\cos(\theta_m + \theta_n) + 1}{(\omega_m + \omega_n)^\gamma}. \quad (16)$$

We introduce the dimensionless temperature:

$$\tau = \frac{2\pi T}{g}. \quad (17)$$

The free energy density  $f$  for a given field configuration is:

$$f = \nu_0 T H_s,$$

where  $\nu_0$  is the density of states at the Fermi level. We define the total free energy functional as:

$$F(\{\theta_m\}) \equiv \frac{2f(\{\theta_m\})}{g^2 \nu_0}, \quad (18)$$

which, in terms of the angles  $\theta_m$  and the dimensionless temperature  $\tau$ , becomes:

$$F(\{\theta_m\}) = -2\tau^2 \sum_{m=0}^{\infty} (2m+1) \cos \theta_m - \tau^{2-\gamma} \sum_{\substack{n,m=0 \\ n \neq m}}^{\infty} \frac{\cos(\theta_m - \theta_n) - 1}{|\omega_m - \omega_n|^\gamma} + \tau^{2-\gamma} \sum_{n,m=0}^{\infty} \frac{\cos(\theta_m + \theta_n) + 1}{(\omega_m + \omega_n)^\gamma}. \quad (19)$$

To obtain the Hessian matrix at the normal state (i.e.,  $\theta_n = 0$  for all  $n$ ), we compute the second derivative of the free energy functional (19). The resulting Hessian matrix  $\tau^{2-\gamma} \tilde{H}$  has elements:

$$\begin{aligned} \tau^{2-\gamma} \tilde{H}_{nn} &= 2\tau^\gamma (2n+1) \cos \theta_n - 2 \frac{\cos(2\theta_n)}{(2n+1)^\gamma} \\ &+ 2 \left( \sum_{\substack{m=0 \\ m \neq n}}^{\infty} \frac{\cos(\theta_m - \theta_n)}{|m - n|^\gamma} - \sum_{m=0}^{\infty} \frac{\cos(\theta_m + \theta_n)}{(m+n+1)^\gamma} \right). \end{aligned} \quad (20)$$

and for  $m \neq n$ :

$$\tau^{2-\gamma} \tilde{H}_{mn} = -2 \left( \frac{\cos(\theta_m - \theta_n)}{|m - n|^\gamma} + \frac{\cos(\theta_m + \theta_n)}{(m+n+1)^\gamma} \right). \quad (21)$$

Expanding the free energy around the normal state yields:

$$\delta F = F - F_N = 2\tau^{2-\gamma} \sum_{n,m=0}^{\infty} \theta_n H_{nm} \theta_m, \quad (22)$$

where  $F_N$  is the free energy of the normal state, and  $H$  is the linearized Hessian matrix evaluated at  $\theta_n = 0$ . The elements of  $H$  are given by:

$$H_{nn} = (2n+1)\tau^\gamma + 2 \sum_{m=1}^n \frac{1}{m^\gamma} - \frac{1}{(2n+1)^\gamma}, \quad (23)$$

and for  $m \neq n$ :

$$H_{mn} = - \left( \frac{1}{|m-n|^\gamma} + \frac{1}{(m+n+1)^\gamma} \right). \quad (24)$$

These are the Hessian matrix elements we referred to in the equations (1) and (2).

### III. TRUNCATION OF THE HESSIAN MATRIX

In the functional analysis of linear operators on infinite-dimensional Hilbert spaces, the reliability of numerical truncation (the finite section method) is strictly determined by the compactness and boundedness properties of the operator. While *bounded operators* are defined by a finite operator norm and a bounded spectral radius, the differential operators governing most systems in mathematical physics are typically unbounded, possessing eigenvalues that scale asymptotically to infinity [36, 37]. A more fundamental topological distinction concerns *compactness*. A compact operator maps bounded sequences to convergent subsequences, a property which guarantees a purely discrete point spectrum accumulating only at zero. Although unbounded differential operators are non-compact, those defined on bounded domains typically possess a *compact resolvent*, defined as the operator  $R_z = (A - zI)^{-1}$ . As established by the spectral theorem, the compactness of the resolvent ensures that the original unbounded operator  $A$  exhibits a purely discrete spectrum bounded from below, despite the unbounded growth of its eigenvalues [38].

Consequently, the convergence of finite-dimensional approximations (such as matrix truncations) is contingent upon preserving the spectral topology of the underlying operator. For operators with a compact resolvent, such as the stiffness matrix of a fixed-boundary elastic string or a confining potential well, truncation is mathematically well-posed; the Min-Max principle guarantees that the eigenvalues of the finite projection converge variationally to the exact discrete eigenvalues of the operator [39]. Conversely, for operators exhibiting a *continuous spectrum*, characteristic of translationally invariant systems like infinite lattices, free fields, or acoustic scattering, finite-dimensional truncation is topologically ill-posed. In these regimes, the discrete eigenvalues of the

truncated matrix attempt to approximate a continuous spectral density, resulting in "spectral pollution" or spurious eigenvalues that depend on the truncation dimension  $N$  rather than physical parameters [40].

To this end, we are interested in showing that, at least for the search for negative points in the spectrum, truncation can still work and be mathematically justified. Building on the analytical methods developed in [3], we now establish a robust justification for matrix truncation that is valid for any  $\gamma > 0$ . Our strategy is to analyze the stability of the normal state by examining the Hessian of the free energy. We will show that this infinite-dimensional operator can be transformed into a more convenient mathematical space, where its spectral properties guarantee that a finite matrix approximation is indeed valid.

The stability of the normal state is determined by the second-order variation of the free energy, which defines a quadratic form, or Hessian operator,  $K^{(2)}$ . Its action on the sequence  $\Theta = (\theta_n)$  is given by:

$$\begin{aligned} K^{(2)}(\Theta)_\gamma &= \sum_{n,m} \theta_n H_{nm} \theta_m \\ &= \sum_{n=0}^{\infty} \left[ (2n+1)\tau^\gamma + 2 \sum_{k=1}^n \frac{1}{k^\gamma} \right] \theta_n^2 \\ &\quad - \sum_{\substack{m=0 \\ n \neq m}}^{\infty} \theta_n \left[ \frac{1}{|n-m|^\gamma} + \frac{1}{(n+m+1)^\gamma} \right] \theta_m \end{aligned} \quad (25)$$

This functional is well-defined on the Hilbert space  $\mathcal{H}$  of real sequences that satisfy the condition  $\|\Theta\|_{\mathcal{H}}^2 := \sum_{n=0}^{\infty} (2n+1)\theta_n^2 < \infty$ . While direct analysis in  $\mathcal{H}$  is challenging due to the weighted norm, we can simplify the problem by mapping it to the standard Hilbert space  $\ell^2(\mathbb{N}_0)$  of square-summable sequences. This is achieved through the transformation  $\xi_n := \sqrt{2n+1} \theta_n$ . In terms of the new sequence  $\Xi = (\xi_n)$ , the quadratic form, denoted  $Q_\gamma(\Xi)$ , becomes:

$$\begin{aligned} Q_\gamma(\Xi) &:= 2K^{(2)}(\Theta)_\gamma = \sum_{n=0}^{\infty} \left[ \tau^\gamma + \frac{2}{2n+1} \sum_{k=1}^n \frac{1}{k^\gamma} \right] \xi_n^2 \\ &\quad - \sum_{\substack{m=0 \\ n \neq m}}^{\infty} \frac{\xi_n}{\sqrt{2n+1}} \left[ \frac{1}{|n-m|^\gamma} + \frac{1}{(n+m+1)^\gamma} \right] \frac{\xi_m}{\sqrt{2m+1}} \end{aligned} \quad (26)$$

A superconducting instability corresponds to  $K_\gamma^{(2)} < 0$ . Since this transformation preserves the sign of the functional, this condition is equivalent to  $Q_\gamma < 0$ . We can therefore analyze the stability of the more tractable operator associated with  $Q_\gamma$ . This functional can be written as  $Q_\gamma(\Xi) = \langle \Xi | \tau^\gamma \tilde{X} | \Xi \rangle$ , where  $\tilde{X} = \mathcal{I} - \tau^{-\gamma} \mathcal{B}$ ,  $\mathcal{I}$  is the identity operator, and the operator  $\mathcal{B}$  is expressed as

$\mathcal{B} = -\mathcal{B}_1 + \mathcal{B}_2 + \mathcal{B}_3$ , whose components are given by:

$$(\mathcal{B}_1(\gamma)\Xi)_n = \left[ \frac{2}{2n+1} \sum_{k=1}^n \frac{1}{k^\gamma} \right] \xi_n, \quad (27)$$

$$(\mathcal{B}_2(\gamma)\Xi)_n = \sum_{m \neq n} \frac{1}{\sqrt{2n+1}} \frac{1}{|n-m|^\gamma} \frac{\xi_m}{\sqrt{2m+1}}, \quad (28)$$

$$(\mathcal{B}_3(\gamma)\Xi)_n = \sum_{m=0}^{\infty} \frac{1}{\sqrt{2n+1}} \frac{1}{(n+m+1)^\gamma} \frac{\xi_m}{\sqrt{2m+1}}. \quad (29)$$

The key insight from [3] is that each of the operators  $\mathcal{B}_i$  for  $i \in \{1, 2, 3\}$  is a *compact operator* on  $\ell^2$ . This property is crucial, as it implies that their sum,  $\mathcal{B}$ , is also compact. A compact operator is, in essence, an infinite-dimensional matrix whose influence effectively vanishes for large indices, meaning it can be arbitrarily well-approximated by a finite-rank matrix. The full operator  $\tilde{X}$  is the sum of a simple self-adjoint operator,  $\mathcal{I}$ , and the compact operator  $-\mathcal{B}$ . By Weyl's theorem [41] on the essential spectrum, the addition of a compact operator does not alter the essential spectrum of a self-adjoint operator. The essential spectrum of  $\mathcal{I}$  is simply the set  $\{1\}$ , and thus  $\sigma_{\text{ess}}(\tilde{X}) = \{1\}$ .

Since the full spectrum is the union of the essential and discrete spectra,  $\sigma(\tilde{X}) = \sigma_{\text{ess}}(\tilde{X}) \cup \sigma_{\text{disc}}(\tilde{X})$ , any eigenvalue that could cross zero to signal an instability must belong to the *discrete spectrum*. The discrete spectrum is generated by the compact part of the operator,  $-\tau^{-\gamma}\mathcal{B}$ . This provides the rigorous basis for our approximation: the search for an instability is equivalent to finding the largest discrete eigenvalue of  $\tau^{-\gamma}\mathcal{B}$  and determining when it exceeds 1. Because these critical eigenvalues are in the discrete spectrum of a compact operator, they can be found by truncating  $\tau^{-\gamma}\mathcal{B}$  to a finite  $N \times N$  matrix,  $\mathcal{B}_N$ , and calculating its eigenvalues numerically. We also notice that finding  $\tau$  for a finite truncation of this compact operator has an eigenvalue greater than 1 is equivalent to a finite truncation of  $\tilde{X}$  has a negative eigenvalue. Since  $\tilde{X}$  is bounded, the only issue we need to worry about is the essential spectrum, which is only  $\{1\}$ , thus contains no negative values. Finally, we note that the original Hessian operator  $H$  is related to  $\tilde{X}$  by the congruence transformation  $H = D\tilde{X}D$ , where  $D$  is the invertible diagonal matrix with entries  $D_{nn} = 1/\sqrt{2n+1}$ . This transformation preserves the signs of the eigenvalues since  $D$  is a diagonal positive definite matrix. Therefore,  $H$  has a zero or negative eigenvalue if and only if  $\tilde{X}$  does. This completes the justification for using a finite Hessian matrix truncation to find the stability threshold for any  $\gamma > 0$ .

#### IV. LOWER BOUNDS

In this section, we establish the lower bounds on  $T_c$  in closed analytical form. To this end, we invoke the well-known *Cauchy's Eigenvalue Interlacing Theorem*[42], stated without proof as follows:

**Eigenvalue Interlacing Theorem:** Suppose  $A \in \mathbb{R}^{n \times n}$  is symmetric. Let  $B \in \mathbb{R}^{m \times m}$  with  $m < n$  be a principal submatrix (obtained by deleting both  $n-m$  rows and  $n-m$  columns). Suppose  $A$  has eigenvalues  $\lambda_1 \leq \dots \leq \lambda_n$  and  $B$  has eigenvalues  $\beta_1 \leq \dots \leq \beta_m$ . Then

$$\lambda_k \leq \beta_k \leq \lambda_{k+n-m} \quad \text{for } k = 1, \dots, m.$$

In particular, if  $m = n-1$ , then the eigenvalues interlace as follows:

$$\lambda_1 \leq \beta_1 \leq \lambda_2 \leq \beta_2 \leq \dots \leq \beta_{n-1} \leq \lambda_n.$$

For any matrix  $H^{(N)}$ , the matrix  $H^{(N-1)}$  is a principal submatrix obtained by removing the  $N$ -th row and column.

Let  $\lambda_1^{(N)}$  denote the smallest eigenvalue of  $H^{(N)}$ . Then, by successively applying the interlacing property, we obtain the following chain of inequalities:

$$\lambda = \lambda_1^\infty \leq \dots \leq \lambda_1^{(4)} \leq \lambda_1^{(3)} \leq \lambda_1^{(2)} \leq \lambda_1^{(1)}. \quad (30)$$

Thus, if  $\lambda_1^{(k)} < 0$  for some  $k$ , it provides a sufficient condition for  $\lambda_1^{(k+1)} < 0$  and hence for the eigenvalue  $\lambda < 0$  of the full infinite matrix as well.

#### A. The Bound $\tau_{c,1}$

The matrix  $H^{(1)}$  consists of a single element, which is also its only eigenvalue. Therefore,

$$\lambda_1^{(1)} < 0 \quad \Rightarrow \quad \tau^\gamma - 1 < 0 \quad \Rightarrow \quad \tau < 1, \quad (31)$$

which yields the bound

$$\tau_{c,1} = 1. \quad (32)$$

#### B. The Bound $\tau_{c,2}$

For convenience, we introduce the substitution  $z = \tau^\gamma$ . The  $2 \times 2$  matrix  $H^{(2)}$  is given by

$$H^{(2)} = \begin{bmatrix} H_{00} & H_{01} \\ H_{10} & H_{11} \end{bmatrix} = \begin{bmatrix} z-1 & -a \\ -a & 3z+2-b \end{bmatrix}, \quad (33)$$

where  $a = (1 + \frac{1}{2\gamma})$  and  $b = \frac{1}{3\gamma}$ .

The condition  $\lambda_1^{(2)} < 0$  leads to the inequality

$$\tau < \left[ \frac{1}{6} \left( 1 + b + \sqrt{25 + 12a^2 - 10b + b^2} \right) \right]^{1/\gamma}. \quad (34)$$

Thus,

$$\tau_{c,2}^\gamma = \frac{1}{6} \left( \left( 1 + \frac{1}{3\gamma} \right) + \sqrt{12 \left( 1 + \frac{1}{2\gamma} \right)^2 + \left( 5 - \frac{1}{3\gamma} \right)^2} \right). \quad (35)$$

which coincides with Eq. (18) in [3].

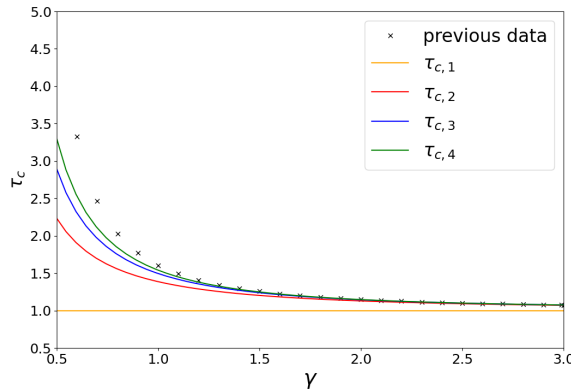


FIG. 2. Comparison of the first four lowest bounds  $\tau_{c,1}, \tau_{c,2}, \tau_{c,3}, \tau_{c,4}$  versus  $\gamma$ , plotted alongside previous numerical solutions of the generalized Eliashberg equations from [31] (black crosses). The plot illustrates the convergence behavior of the bounds as  $\gamma$  increases, with each successive bound providing a tighter estimate of  $\tau_c$ .

### C. Higher Bounds $\tau_{c,N}$

The higher lower bounds  $\tau_{c,N}$  are obtained in the same way. This equivalent to solving the polynomial equation in  $z = \tau^\gamma$  of the  $N^{\text{th}}$  degree:

$$\det(H^{(N)}) = 0. \quad (36)$$

The transition temperature bound is the lowest positive solution to this equation. In principle, the 3<sup>rd</sup> and 4<sup>th</sup> bounds can be obtained in a closed form. Any  $n \geq 5$ , requires numerical solutions, as generally no closed form exists. The first four bounds on the transition temperature are summarized in Fig. 2.

To investigate the effect of the truncation size, we plot the temperatures for different truncations  $N = 100, 400, 1000$  in Fig. 3. We see that for  $\gamma \geq 0.5$ , the lowest truncation  $N = 100$  works reasonably well. In the region  $0 < \gamma < 0.5$ , we clearly see that the obtained temperature depends strongly on the truncation size. This is consistent with the condition  $(N\tau)^\gamma \ll 1$ .

## V. UPPER BOUND

In the previous section, we determined the lower bound for the transition temperature. In this section, we establish the upper bound for the  $T_c$ .

We will use the well-known *Gershgorin Circle Theorem* [43] to determine the lowest value of  $\tau$  for which all eigenvalues of the matrix are positive. The theorem is stated as follows:

**Gershgorin Circle Theorem** Let  $H^{(N)} = (h_{ij})$  be a square  $N \times N$  matrix. For each  $i = 1, \dots, n$ , define the

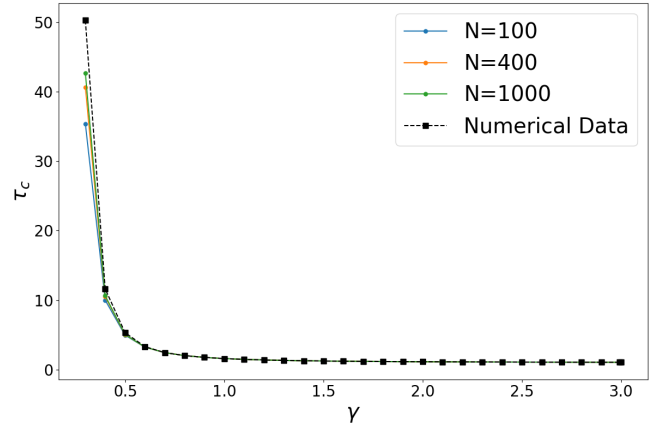


FIG. 3. The transition temperature  $\tau_c$  is plotted vs  $\gamma$  for different truncation values  $N = 100, 400, 1000$ . for  $\gamma \geq 0.5$ , all truncation levels agree well with the previous numerical solutions of generalized Eliashberg equations [31]. As  $\gamma \rightarrow 0$ ,  $\tau_c \rightarrow \infty$  as expected, which shows that the optimal truncation  $N \rightarrow \infty$ . All lower truncation levels serve as a "lower bound".

*Gershgorin disc*  $d_i$  centered at  $h_{ii}$  with radius

$$R_i = \sum_{\substack{j=1 \\ j \neq i}}^n |h_{ij}|.$$

Then each eigenvalue  $\lambda$  of  $H^{(N)}$  lies within at least one of the discs:

$$\lambda \in \bigcup_{i=1}^N d_i = \bigcup_{i=1}^N \{x \in \mathbb{C} : |x - h_{ii}| \leq R_i\}.$$

For the detailed proof, we refer the reader to [42–44]. We notice also that the proof holds for  $N \rightarrow \infty$  under two conditions. First, the existence of a discrete eigenvalue, which we have argued in Sec. III that it's indeed the case, and second, that the entries of the eigenvectors, i.e  $\theta_n$ , are bounded. Crucially, the theorem does not imply that every individual disc contains an eigenvalue. Rather, it asserts that every eigenvalue is contained within at least one disc; stated more rigorously, the complete spectrum of the matrix lies within the union of all the discs.

A key advantage of the Gershgorin circle theorem is its broad applicability. Unlike the eigenvalue interlacing, which is restricted to Hermitian or symmetric matrices, the Gershgorin theorem applies to any square matrix with real or complex entries. This makes it a highly versatile tool for estimating the location of eigenvalues in a wide variety of contexts. The theorem provides two ways to construct the disks that contain the eigenvalues: one based on rows and another on columns. For any given square matrix  $H$ , the *row disks* are centered at the diagonal entries  $h_{ii}$  with radii  $R_i = \sum_{j \neq i} |h_{ij}|$ , while the *column disks* are centered at the same points but with radii  $C_i = \sum_{j \neq i} |h_{ji}|$ . For a non-symmetric matrix, these two sets of disks are generally different, but the theorem still applies to both of them.

### A. Simplest Case

Consider the simplest case where we apply the theorem directly to the Hessian matrix. Recall that the diagonal elements are given by Eq. (23):

$$h_{ii} = (2i+1)\tau^\gamma + 2 \sum_{m=1}^i \frac{1}{m^\gamma} - \frac{1}{(2i+1)^\gamma},$$

and the radii are given by the summation of off-diagonal elements and taking the limit  $N \rightarrow \infty$ :

$$R_i = 2 \sum_{j=1}^{\infty} \frac{1}{j^\gamma} - \frac{1}{(2i+1)^\gamma}.$$

The term  $\sum_{j=1}^{\infty} \frac{1}{j^\gamma} = \zeta(\gamma)$  for  $\gamma > 1$  and diverges otherwise. It follows that each disc  $d_i$  is bounded from below by:

$$(2i+1)\tau^\gamma + 2 \sum_{m=1}^i \frac{1}{m^\gamma} - 2 \sum_{j=1}^{\infty} \frac{1}{j^\gamma} \leq d_i^\downarrow. \quad (37)$$

For example:

$$d_0^\downarrow \geq \tau^\gamma - 2 \sum_{j=1}^{\infty} \frac{1}{j^\gamma},$$

$$d_1^\downarrow \geq 3\tau^\gamma + 2 - 2 \sum_{j=1}^{\infty} \frac{1}{j^\gamma},$$

$$d_2^\downarrow \geq 5\tau^\gamma + 2 \left(1 + \frac{1}{2^\gamma}\right) - 2 \sum_{j=1}^{\infty} \frac{1}{j^\gamma}, \quad \text{and so on.}$$

It is evident that for any  $\tau \geq 0$ , the lower bound of  $d_0$  is the smallest among all  $d_i$ , and thus serves as a lower bound for the union of all Gershgorin discs.

To ensure that no phase transition occurs, all eigenvalues must be positive. Let  $\lambda_N$  denote the smallest eigenvalue of  $H^{(N)}$  for sufficiently large  $N \rightarrow \infty$ , and suppose  $\lambda_N \approx 0^+$ . Then, by the Gershgorin theorem:

$$\tau^\gamma - 2 \sum_{j=1}^{\infty} \frac{1}{j^\gamma} \leq \lambda_n = 0^+ \Rightarrow \tau^\gamma < 2 \sum_{j=1}^{\infty} \frac{1}{j^\gamma}. \quad (38)$$

This implies the following upper bound for the transition temperature:

$$\tau_c^{\max} = (2\zeta(\gamma))^{\frac{1}{\gamma}}, \quad \gamma > 1. \quad (39)$$

This is the temperature above which all eigenvalues of any  $H$  are positive. The result in Eq. (39) is only valid for  $\gamma > 1$ , and doesn't provide good improvement at values  $\gamma \leq 1.5$ . We propose a new technique to improve this upper bound, while still using Gershgorin Circle Theorem.

### B. Improving the Upper Bound

Since the Gershgorin circle theorem is not restricted to symmetric matrices, we can manipulate our original matrix to obtain another matrix with the same eigenvalues, or at least their respective signs, while tightening the Gershgorin bounds.

We note that as  $\tau$  becomes less than  $\tau_c$  the determinant of the Hessian changes sign. So if instead of the Hessian  $H^{(N)}$  we consider another matrix

$$h^{(N)} = O^{-1} H^{(N)} O \quad (40)$$

where  $O$  is some, say, positive definite  $N \times N$  matrix, then as  $\det h^{(N)} = \det H^{(N)}$ ,  $\tau_c$  — the temperature at which the lowest eigenvalue is zero — is the same for both  $h^{(N)}$  and  $H^{(N)}$ .

We then can choose the matrix  $O$ .

Let's take  $O$  in the form  $O = \text{diag}(1/p, 1/(1+p), \dots, 1/(n+p), \dots, 1/(N+p-1))$ , where  $0 < p < 1$  is some tunable parameter.

The matrix elements of  $h^{(N)}$  are

$$h_{nn} = H_{nn} = (2n+1)\tau^\gamma + 2 \sum_{m=1}^n \frac{1}{m^\gamma} - \frac{1}{(2n+1)^\gamma} \quad (41)$$

$$\begin{aligned} h_{mn} &= (m+p)H_{mn} \frac{1}{n+p} \\ &= -(m+p) \left( \frac{1}{|m-n|^\gamma} + \frac{1}{(m+n+1)^\gamma} \right) \frac{1}{n+p} \end{aligned} \quad (42)$$

The Gershgorin radii are

$$\begin{aligned} R_m^{(N)} &= \sum_{\substack{n=0 \\ n \neq m}}^N |h_{mn}| \\ &= (m+p) \sum_{\substack{n=0 \\ n \neq m}}^N \left( \frac{1}{|m-n|^\gamma} + \frac{1}{(m+n+1)^\gamma} \right) \frac{1}{n+p} \end{aligned} \quad (43)$$

Then we can take the limit  $N \rightarrow \infty$ , as the sum converges for any  $\gamma > 0$ . The problem becomes an optimization problem for the parameter  $p$ . Also, it's worth noting here that we can no longer assume that the zeroth Gershgorin disc is the lowest disc and use it to calculate the upper bound. In the appendix, we show that indeed for some values of  $p$ , the zeroth disc isn't the lowest. However, we prove in the appendix that for  $p = 1/2$ , the zeroth disc is the lowest disc for any  $\gamma > 0$ . Thus, we use the zeroth disc to compute the upper bound by setting  $p = 1/2$ .

Thus, for  $p = 1/2$ , the expression for the upper bound is given by

$$\begin{aligned} \tau_{\text{up}}^\gamma &= \frac{1}{2} \sum_{n=1}^{\infty} \frac{1}{n^\gamma} \frac{2n}{(n+1/2)(n-1/2)} \\ &= \sum_{n=0}^{\infty} \left( \frac{1}{2} \right)^{2n} \zeta(\gamma + 2n + 1) \end{aligned} \quad (44)$$

Which converges for any  $\gamma > 0$ . The comparison of our results against the numerical values and Kiessling et. al's upper bound is plotted in Fig. 4.

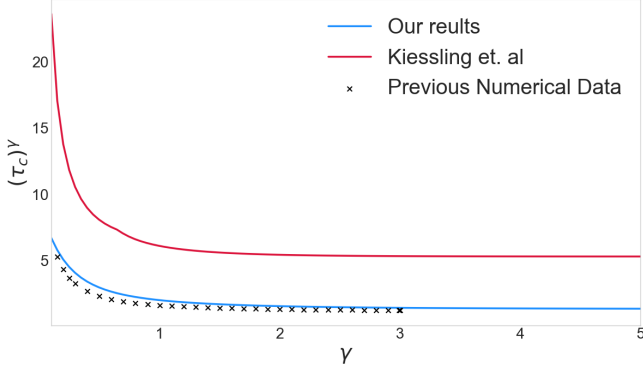


FIG. 4. Comparison of our results (blue line) for the upper bound of the critical temperature obtained from Eq. 44 as a function of  $\gamma$  in the range  $0.1 \leq \gamma \leq 5$  compared to the numerical data (black crosses) from [31] in comparison to the Upper bound obtained by Kiessling et. al [3] (red line). Our results show a significant improvement in the upper bound. Note that we are plotting  $\tau_c^\gamma$  to be able to fit both bounds in the same plot.

## VI. SUMMARY AND CONCLUSION

This paper formally addresses the problem of determining the critical transition temperatures in the  $\gamma$ -model of quantum-critical superconductivity by performing a linear stability analysis of the Hessian matrix of the free energy functional obtained through mapping the theory into a classical spin chain. The primary challenge is that the Hessian is an infinite-dimensional operator that is not bounded, and consequently non-compact, as the diagonal elements  $H_{nn} \rightarrow \infty$  as  $n \rightarrow \infty$ . This means that a truncation to a finite matrix is not straightforward, mathematically speaking, and needs to be rigorously justified.

To establish the validity of truncating the infinite Hessian matrix, we argued that it is possible by employing a congruence transformation to recast the unbounded Hessian,  $H$ , into a new, bounded operator,  $\tilde{X}$ , on the Hilbert space  $\ell^2$ . This transformation preserves the signs of the eigenvalues. The structure of  $\tilde{X}$  as a simple term plus a compact operator, combined with Weyl's theorem, guarantees that any instability must arise from a discrete, negative eigenvalue. We argued that this justifies reducing the search for the transition temperature to the tractable problem of diagonalizing a finite  $N \times N$  matrix with the limit  $N \rightarrow \infty$ .

With the truncation justified, we derived rigorous bounds for the first transition temperature. To establish lower bounds, we applied the Interlacing Eigenvalue Theorem [42]. This theorem guarantees that the lowest

eigenvalue of any  $N \times N$  truncation is greater than or equal to that of the  $(N + 1) \times (N + 1)$  truncation, creating a monotonically increasing sequence of transition temperatures that converges from below. By solving for the transition temperatures of the  $N = 1, 2, 3$ , and 4 truncations, we obtained a sequence of increasingly tight lower bounds. These results provide an independent confirmation of the findings of Kiessling et al. [3], which were derived using variational principles.

To establish upper bounds, we employed the Gershgorin Circle Theorem [43, 44], which provides a region in the complex plane guaranteed to contain all eigenvalues. An upper bound on the transition temperature is found by determining the temperature at which the lowest Gershgorin disk touches zero. To tighten this bound, we applied an optimized similarity transformation using a diagonal matrix  $O$  parameterized by a single variable,  $p$ . Through an analytical optimization, we found the optimal value  $p = 1/2$  that minimizes the resulting upper bound on the temperature. This procedure yielded a new, closed-form expression for the upper bound that represents a significant improvement of the results of Kiessling et al. [3] and converges much more rapidly to the numerical transition temperature obtained from solving the coupled Eliashberg equations [31]. Our results, in comparison to numerical data and current bounds in the literature are summarized in Fig. (1) in the introduction section.

## ACKNOWLEDGMENTS

We thank Yi-Ming Wu for sharing the numerical results from [31]. We also thank Michael K-H Kiessling for sharing some of the numerical data from [3].

## Appendix A: Calculating the Optimal $p$

Computing the lower boundaries of the Gershgorin discs  $d_m^\downarrow$ , we have:

$$d_{m=0}^\downarrow = \tau^\gamma - p \sum_{n=1}^{\infty} \frac{1}{n^\gamma} \left( \frac{1}{n+p} + \frac{1}{n+p-1} \right) \quad (A1)$$

$$\begin{aligned} d_{m>0}^\downarrow = & (2m+1)\tau^\gamma \\ & + \sum_{n=1}^m \frac{1}{n^\gamma} \left( 2 - \frac{m+p}{m-n+p} - \frac{m+p}{m+n+p} \right) \\ & - (m+p) \sum_{n=m+1}^{\infty} \frac{1}{n^\gamma} \left( \frac{1}{n+m+p} + \frac{1}{n-m+p-1} \right) \end{aligned} \quad (A2)$$

Now we introduce the temperature  $\tau_m$  at which the  $m$ th Gershgorin disk touches zero.

$$\tau_0^\gamma = p \sum_{n=1}^{\infty} \frac{1}{n^\gamma} \left( \frac{1}{n+p} + \frac{1}{n+p-1} \right), \quad (\text{A3})$$

$$\begin{aligned} \tau_{m>0}^\gamma &= \frac{1}{2m+1} \sum_{n=1}^m \frac{1}{n^\gamma} \frac{2n^2}{(m+p)^2 - n^2} \\ &+ \frac{(m+p)}{2m+1} \sum_{n=m+1}^{\infty} \frac{1}{n^\gamma} \frac{2n+p-1}{(n+m+p)(n-m+p-1)}. \end{aligned} \quad (\text{A4})$$

The true upper bound  $\tau_u$  for  $\tau_c$  for given  $p$  is then

$$\tau_u^\gamma = \max_m \tau_m^\gamma. \quad (\text{A5})$$

Unlike the simplest case, it's not clear whether the zeroth disc  $d_0$  is the lowest of all the discs for any value of  $p$ . In Fig. 5, we plot the temperature  $\tau_0^\gamma$  vs  $\gamma$  for different values of  $p$ . We immediately see that for some values of  $p$ , the "upper bound  $\tau_0$ " is lower than the numerical data, indicating that the assumption that the zeroth disc is the lowest one is no longer true. This statement is also obtained from the numerical comparison of  $\tau_m^\gamma$  at different  $p$ .

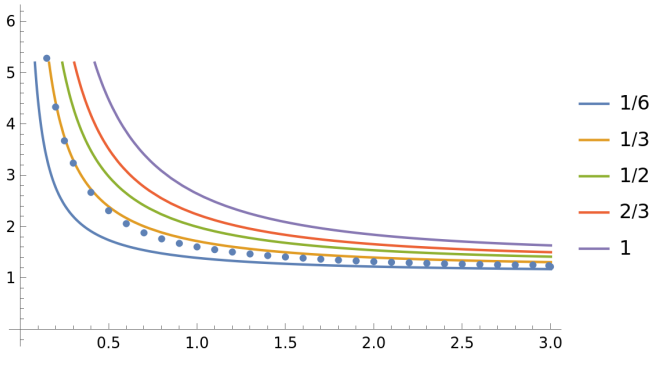


FIG. 5. The upper bound  $\tau_0^\gamma$  vs  $\gamma$  for different values of  $p$  shown as legends. Dots are the numerical data. It's clear that for  $p = 1/6$ , the upper bound is below the data. It indicates that somewhere  $1/2 < p < 1/3$ , the assumption that the zeroth Gershgorin disc is the lowest is no longer valid.

However, for  $p = 1/2$ , we show that  $\tau_0^\gamma - \tau_{m>0}^\gamma \geq 0$  for any  $m$  and is zero for  $\gamma = 0$ . For  $p = 1/2$  the equations

(A3) and (A4) give

$$\tau_0^\gamma = \frac{1}{2} \sum_{n=1}^{\infty} \frac{1}{n^\gamma} \frac{2n}{(n+1/2)(n-1/2)} \quad (\text{A6})$$

$$\begin{aligned} \tau_{m>0}^\gamma &= -\frac{2}{2m+1} \sum_{n=1}^m \frac{1}{n^\gamma} + \frac{1}{2} \sum_{n=1}^{\infty} \frac{1}{n^\gamma} \frac{1}{n+m+1/2} \\ &- \frac{1}{2} \sum_{n=1}^{\infty} \frac{1}{n^\gamma} \frac{1}{n-m-1/2} + \sum_{n=1}^{\infty} \frac{1}{(n+m)^\gamma} \frac{1}{n-1/2} \end{aligned} \quad (\text{A7})$$

The quantity  $\tau_0^\gamma - \tau_{m>0}^\gamma$  can be written in the following form

$$\begin{aligned} \tau_0^\gamma - \tau_{m>0}^\gamma &= \frac{1}{2} \sum_{n=1}^m \frac{1}{n^\gamma} \frac{2}{m+1/2} \\ &- \frac{1}{2} \sum_{n=1}^m \frac{1}{n^\gamma} \frac{1}{m+1/2-n} + \frac{1}{2} \sum_{n=1}^m \frac{1}{n^\gamma} \frac{1}{n+1/2} \\ &+ \frac{1}{2} \sum_{n=1}^{\infty} \left( \frac{1}{n^\gamma} - \frac{1}{(n+m)^\gamma} \right) \left( \frac{1}{n-1/2} - \frac{1}{n+m+1/2} \right) \end{aligned} \quad (\text{A8})$$

The last line of this equality is obviously non-negative (it is zero for  $\gamma = 0$ ). Let's consider the first and the second lines. They can be written in the following form

$$\begin{aligned} &\frac{1}{2} \sum_{n=1}^m \frac{1}{n^\gamma} \frac{2}{m+1/2} \\ &- \frac{1}{2} \sum_{n=1}^m \frac{1}{n^\gamma} \frac{1}{m+1/2-n} + \frac{1}{2} \sum_{n=1}^m \frac{1}{n^\gamma} \frac{1}{n+1/2} \\ &= \frac{1}{2} \sum_{n=1}^{m-1} \left( \frac{1}{n^\gamma} - \frac{1}{(m-n)^\gamma} \right) \frac{1}{n+1/2} \\ &+ \frac{1}{m+1/2} \sum_{n=1}^m \left( \frac{1}{n^\gamma} - \frac{1}{m^\gamma} \right) \end{aligned} \quad (\text{A9})$$

The last term is obviously non-negative (it is zero for  $m = 1$  or  $\gamma = 0$ ), so let's concentrate on the first term. It can be written in the following form

$$\begin{aligned} &\frac{1}{2} \sum_{n=1}^{m-1} \left( \frac{1}{n^\gamma} - \frac{1}{(m-n)^\gamma} \right) \frac{1}{n+1/2} \\ &= \frac{1}{4} \sum_{n=1}^{m-1} \frac{((m-n)^\gamma - n^\gamma)(m-2n)}{n^\gamma(m-n)^\gamma(n+1/2)(m-n+1/2)} \end{aligned} \quad (\text{A10})$$

The denominator in the expression under the sum is positive. In the numerator, there are two factors  $(m-n)^\gamma - n^\gamma$  and  $m-2n$ . For  $0 < n < m$ , these two factors always have the same sign: positive if  $n < m/2$  and negative if  $n > m/2$  (if  $m$  is even and  $n = m/2$ , then both factors are zero). So, this sum is also non-negative (it is zero if  $m = 2$  or  $\gamma = 0$ ). So, taking all this together, this proves that  $\tau_0^\gamma - \tau_{m>0}^\gamma$  is non-negative for any  $m$  and is zero for  $\gamma = 0$ .

---

[1] E. A. Yuzbashyan and B. L. Altshuler, Migdal-Eliashberg theory as a classical spin chain, *Physical Review B* **106**, 10.1103/physrevb.106.014512 (2022).

[2] E. A. Yuzbashyan, M. K.-H. Kiessling, and B. L. Altshuler, Superconductivity near a quantum critical point in the extreme retardation regime, *Physical Review B* **106**, 10.1103/physrevb.106.064502 (2022).

[3] M. K.-H. Kiessling, B. L. Altshuler, and E. A. Yuzbashyan, Bounds on  $T_c$  in the Eliashberg theory of superconductivity. I: The  $\gamma$ -model, *Journal of Statistical Physics* **192**, 10.1007/s10955-025-03446-5 (2025).

[4] H. K. Onnes, Further experiments with liquid helium. C. on the change of electric resistance of pure metals at very low temperatures etc. IV. the resistance of pure mercury at helium temperatures, *KNAW Proceedings* **13**, 1274 (1911).

[5] H. K. Onnes, The liquefaction of helium, *Communications from the Physical Laboratory at Leiden* (1908), also published in *Proceedings of the Royal Netherlands Academy of Arts and Sciences*, 11, 168-185 (1909).

[6] W. Meissner and R. Ochsenfeld, Ein neuer Effekt bei Eintritt der Supraleitfähigkeit, *Naturwissenschaften* **21**, 787 (1933).

[7] J. Bardeen, L. N. Cooper, and J. R. Schrieffer, Theory of superconductivity, *Phys. Rev.* **108**, 1175 (1957).

[8] L. N. Cooper, Bound Electron Pairs in a Degenerate Fermi Gas, *Phys. Rev.* **104**, 1189 (1956).

[9] C. A. Reynolds, B. Serin, W. H. Wright, and L. B. Nesbitt, Superconductivity of isotopes of mercury, *Phys. Rev.* **78**, 487 (1950).

[10] E. Maxwell, Isotope effect in the superconductivity of mercury, *Phys. Rev.* **78**, 477 (1950).

[11] A. B. Migdal, Interaction between electrons and lattice vibrations in a normal metal, *Soviet Physics JETP* **7**, 996 (1958).

[12] G. Eliashberg, Interactions between electrons and lattice vibrations in a superconductor, *SOVIET PHYSICS JETP* **11** (1960).

[13] G. Eliashberg, Temperature green's function for electrons in a superconductor, *SOVIET PHYSICS JETP* **12** (1961).

[14] J. G. Bednorz and K. A. Müller, Possible high  $T_c$  superconductivity in the Ba-La-Cu-O system, *Zeitschrift für Physik B Condensed Matter* **64**, 189 (1986).

[15] A. Schilling, M. Cantoni, J. D. Guo, and H. R. Ott, Superconductivity above 130 k in the Hg-Ba-Ca-Cu-O system, *Nature* **363**, 56 (1993).

[16] D. J. Scalapino, The case for  $d_{x^2-y^2}$  pairing in the cuprate superconductors, *Physics Reports* **250**, 329 (1995).

[17] Y. Kamihara, T. Watanabe, M. Hirano, and H. Hosono, Iron-based layered superconductor  $\text{La}[\text{o}_{1-x}\text{f}_x]\text{feas}$  ( $x = 0.05-0.12$ ) with  $t_c = 26$  k, *Journal of the American Chemical Society* **130**, 3296 (2008).

[18] G. R. Stewart, Heavy-fermion systems, *Reviews of Modern Physics* **56**, 755 (1984).

[19] J. A. Hertz, Quantum critical phenomena, *Physical Review B* **14**, 1165 (1976).

[20] P. Monthoux, A. V. Balatsky, and D. Pines, Toward a theory of high-temperature superconductivity in the antiferromagnetically correlated cuprates, *Physical Review B* **46**, 14803 (1992).

[21] D. J. Scalapino, A common thread: The pairing interaction for unconventional superconductors, *Reviews of Modern Physics* **84**, 1383 (2012).

[22] A. V. Chubukov, Pairing in 'gamma-models' for quantum-critical metals, *Annalen der Physik* **532**, 2000219 (2020).

[23] A. Abanov, A. V. Chubukov, and J. Schmalian, Quantum-critical theory of the spin-fermion model and its application to cuprates: Normal state analysis, *Advances in Physics* **52**, 119 (2003).

[24] E.-G. Moon and A. Chubukov, Quantum-critical pairing with varying exponents, *Journal of Low Temperature Physics* **161**, 263 (2010).

[25] A. Abanov and A. V. Chubukov, Interplay between superconductivity and non-Fermi liquid at a quantum critical point in a metal. I. the  $\gamma$  model and its phase diagram at  $T = 0$ : The case  $0 < \gamma < 1$ , *Physical Review B* **102**, 024524 (2020).

[26] Y.-M. Wu, A. Abanov, Y. Wang, and A. V. Chubukov, Interplay between superconductivity and non-Fermi liquid at a quantum critical point in a metal. II. the  $\gamma$  model at a finite  $T$  for  $0 < \gamma < 1$ , *Physical Review B* **102**, 024525 (2020).

[27] Y.-M. Wu, A. Abanov, and A. V. Chubukov, Interplay between superconductivity and non-Fermi liquid behavior at a quantum critical point in a metal. III. the  $\gamma$  model and its phase diagram across  $\gamma = 1$ , *Physical Review B* **102**, 094516 (2020).

[28] Y.-M. Wu, S.-S. Zhang, A. Abanov, and A. V. Chubukov, Interplay between superconductivity and non-Fermi liquid at a quantum critical point in a metal. IV. the  $\gamma$  model and its phase diagram at  $1 < \gamma < 2$ , *Physical Review B* **103**, 024522 (2021).

[29] Y.-M. Wu, S.-S. Zhang, A. Abanov, and A. V. Chubukov, Interplay between superconductivity and non-Fermi liquid behavior at a quantum-critical point in a metal. V. the  $\gamma$  model and its phase diagram: The case  $\gamma = 2$ , *Physical Review B* **103**, 184508 (2021).

[30] S.-S. Zhang, Y.-M. Wu, A. Abanov, and A. V. Chubukov, Interplay between superconductivity and non-Fermi liquid at a quantum critical point in a metal. VI. the  $\gamma$  model and its phase diagram at  $2 < \gamma < 3$ , *Physical Review B* **104**, 144509 (2021).

[31] Y.-M. Wu, A. Abanov, Y. Wang, and A. V. Chubukov, Special role of the first Matsubara frequency for superconductivity near a quantum critical point: Nonlinear gap equation below  $T_c$  and spectral properties in real frequencies, *Physical Review B* **99**, 144512 (2019).

[32] M. K.-H. Kiessling, B. L. Altshuler, and E. A. Yuzbashyan, Bounds on  $T_c$  in the Eliashberg theory of superconductivity. II: Dispersive phonons, arXiv preprint (2024), arXiv:2409.00532.

[33] M. K.-H. Kiessling, B. L. Altshuler, and E. A. Yuzbashyan, Bounds on  $T_c$  in the Eliashberg theory of superconductivity. III: Einstein phonons, arXiv preprint (2024), arXiv:2409.02121.

[34] Y. Wang, A. Abanov, B. L. Altshuler, E. A. Yuzbashyan, and A. V. Chubukov, Superconductivity near a quantum-critical point: The special role of the first Matsubara frequency, *Physical Review Letters* **117**, 157001 (2016).

- [35] A. V. Chubukov, A. Abanov, I. Esterlis, and S. A. Kivelson, Eliashberg theory of phonon-mediated superconductivity—when it is valid and how it breaks down, *Annals of Physics* **417**, 168190 (2020).
- [36] T. Kato, *Perturbation Theory for Linear Operators*, 2nd ed., Classics in Mathematics, Vol. 132 (Springer, Berlin, 1995).
- [37] I. J. Maddox, *Elements of Functional Analysis* (Cambridge University Press, New York, 1970).
- [38] M. Reed and B. Simon, *Methods of Modern Mathematical Physics I: Functional Analysis* (Academic Press, New York, 1980).
- [39] R. Courant and D. Hilbert, *Methods of Mathematical Physics, Vol. I* (Interscience Publishers, New York, 1953).
- [40] A. Böttcher and B. Silbermann, *Introduction to Large Truncated Toeplitz Matrices* (Springer, New York, 1999).
- [41] H. Weyl, Über gewöhnliche Differentialgleichungen mit Singularitäten und die zugehörigen Entwicklungen willkürlicher Funktionen, *Mathematische Annalen* **68**, 220 (1909).
- [42] R. A. Horn and C. R. Johnson, *Matrix Analysis*, 2nd ed. (Cambridge University Press, 2012).
- [43] S. Gershgorin, Über die Abgrenzung der Eigenwerte einer Matrix, *Bulletin de l'Académie des Sciences de l'URSS. Classe des sciences mathématiques et naturelles* **6**, 749 (1931).
- [44] R. S. Varga, *Gershgorin and His Circles*, Springer Series in Computational Mathematics, Vol. 36 (Springer-Verlag, 2004).